

ReAugment: Model Zoo-Guided RL for Few-Shot Time Series Augmentation and Forecasting

Haochen Yuan¹ Yutong Wang¹ Yihong Chen¹ Yunbo Wang^{1*} Xiaokang Yang¹

¹MoE Key Lab of Artificial Intelligence, AI Institute, Shanghai Jiao Tong University
{yuanhaochen, yunbow}@sjtu.edu.cn

Abstract

Time series forecasting, particularly in few-shot learning scenarios, is challenging due to the limited availability of high-quality training data. To address this, we present a pilot study on using reinforcement learning (RL) for time series data augmentation. Our method, ReAugment, tackles three critical questions: which parts of the training set should be augmented, how the augmentation should be performed, and what advantages RL brings to the process. Specifically, our approach maintains a forecasting model zoo, and by measuring prediction diversity across the models, we identify samples with higher probabilities for overfitting and use them as the anchor points for augmentation. Leveraging RL, our method adaptively transforms the *overfit-prone* samples into new data that not only enhances training set diversity but also directs the augmented data to target regions where the forecasting models are prone to overfitting. We validate the effectiveness of ReAugment across a wide range of base models, showing its advantages in both standard time series forecasting and few-shot learning tasks.

1 Introduction

Time series forecasting is a critical task with diverse applications, but it faces significant challenges due to the limited availability of high-quality training data. This challenge is further amplified in time-evolving domains with inherent non-stationarity and becomes even more pronounced in few-shot learning scenarios, where the scarcity of data affects the performance of forecasting models. While recent methods have focused on developing deep-learning architectures to capture long-term trends, clinical patterns, and multivariate relationships [33, 23, 21], in this work, we explore a learning-based data augmentation method that can be seamlessly integrated with existing forecasting models.

Effective data augmentation requires generating high-quality, diverse training samples. However, in practice, existing forecasting models typically rely on fixed-form data augmentation techniques [30, 5], which lack data-dependent adaptability and may introduce unexpected noise. Previous learning-based augmentation methods typically involve contrastive learning [8] or Mixup combinations [26] to generate new data sequences. However, these methods are **NOT task-oriented**, as the data generation process is not guided by the performance of the downstream forecasting models. In contrast, we argue that enabling a *closed-loop augmentation-forecasting process* is essential, which requires aligning the training objectives of augmentation models with the resulting forecasting performance.

To achieve this, we present **ReAugment**, which uses reinforcement learning (RL) to enable closed-loop data augmentation and enhance the generalizability of few-shot forecasting models. We aim to answer three critical questions: (1) *Which parts of the training set should be augmented?* (2) *How should the augmentation be performed?* (3) *What advantages does RL offer compared to existing approaches?* Accordingly, ReAugment is designed to dynamically identify a training subset of

*Corresponding author: Yunbo Wang (yunbow@sjtu.edu.cn).

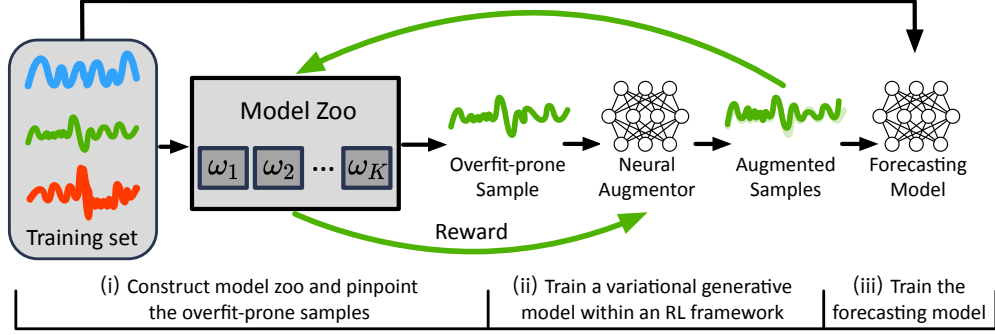


Figure 1: ReAugment enables closed-loop optimization of time series augmentation and forecasting, presenting an early study on using reinforcement learning for (few-shot) time series augmentation.

overfit-prone samples that would benefit most from augmentation and automatically searches for optimal augmentation policies tailored to these samples.

Specifically, ReAugment initially leverages a *forecasting model zoo*, consisting of diverse instances of the same network architecture trained via cross-validation, to identify overfit-prone training samples in need of augmentation. An interesting finding is that training forecasting models exclusively with data samples that present **low prediction variance** across the model zoo often leads to better performance (detailed in Section 3). This insight leads us to select the data points with high prediction variance across the model zoo as the root of the subsequent augmentation process.

Based on the identified overfit-prone samples, ReAugment learns an augmentation network in the form of a *variational masked autoencoder* (VMAE), in which the latent space is used as the action space in the RL framework. The RL-based augmentation policies are guided by a reward function derived from **backtesting the model-zoo errors**, measured by applying the generated data to the forecasting model zoo. The reward function balances both the diversity and quality of the augmented data: It encourages the new data points to fall into regions where the forecasting models tend to overfit, while maintaining alignment with the original data distribution. We employ the REINFORCE algorithm [32] to enable optimization of the VMAE under a non-differentiable reward function.

In summary, we provide a pilot study on leveraging RL for time series augmentation, which demonstrates substantial improvements across a wide range of base models and datasets, especially in few-shot learning scenarios. Key technical contributions of this work are as follows:

- *Finding overfit-prone data as augmentation anchor points:* We propose a novel method for identifying overfit-prone samples by leveraging cross-validation errors from a forecasting model zoo to pinpoint anchor points with potential value for data augmentation.
- *Augmentation model:* We introduce a novel network architecture based on a variational masked autoencoder for sequential data, where the latent space is used as the action space of RL.
- *A pilot study of RL for time series augmentation:* We leverage RL to incorporate a non-differentiable objective into the augmentation process. At the core of this approach is a reward function that uses prediction responses from the model zoo to guide data generation toward regions where forecasting models are likely to overfit.

2 Related Work

Transformer-based time series forecasting. Compared with CNN-based or RNN-based forecasting models [28, 29, 4, 25], recent Transformer-based methods [17, 33, 40, 20, 41, 39, 38, 2, 35] have shown superior performance across a wide range of time series forecasting tasks. Most previous work has focused on developing more effective network architectures to capture long-term trends, clinical patterns, and multivariate relationships within the data. For instance, Autoformer [33] improves upon the Transformer by employing a deep decomposition architecture that progressively separates trend and seasonal components throughout the forecasting process. PatchTST [23] vectorizes time series data into patches of specified size, which are then encoded through a Transformer, with the model producing forecasts of the desired length via an appropriate prediction head. LSTF-Linear [38] simplifies complex time series forecasting problems and outperforms many Transformers by using a set of remarkably simple one-layer linear models. iTransformer [21] modifies the architecture by

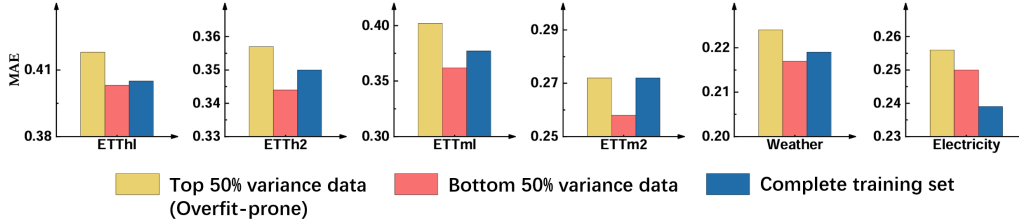


Figure 2: Preliminary findings on overfit-prone data. We compare the performance of *iTransformer* trained with different splits of the original training set, which are divided based on the variance of prediction errors across the forecasting model zoo.

adopting components with inverted dimensions, demonstrating superior performance on multivariate time series data. Unlike these methods, we introduce a data augmentation method that can be broadly combined with existing forecasting models.

Few-shot time series forecasting. In many real-world applications, obtaining sufficient data can be challenging, especially in scenarios where data is scarce, noisy, or difficult to collect [9, 34, 14, 37]. Recent literature has introduced large foundation models specifically designed for time series forecasting [7, 15, 1, 10, 19, 22, 24], often evaluating these models under zero-shot domain generalization settings. However, in preliminary experiments, we found that as the distribution gap between training and testing data increases (*e.g.*, when data comes from different domains), the generalization performance of these models significantly decreases.

Time series augmentation. Iglesias *et al.* [13] have presented a taxonomy of augmentation techniques. Simple augmentation methods involve time, frequency, and magnitude domain transformation techniques such as slicing [3], frequency warping [6], and jittering [11]. The second category is the learning-based methods, including those based on contrastive learning [8], and Mixup combinations [26]. Additionally, advanced generative models have been employed to generate realistic time series data, including the GAN-based [36, 18], VAE-based [27, 16], and Diffusion-based [12] methods. The generated samples can be used for further training of the forecasting models. In contrast to existing approaches, we present a pilot study on using RL for time series data augmentation.

3 Overfit-Prone Samples as Anchor Data

3.1 Finding Overfit-Prone Data with a Model Zoo

The first challenge we need to address is identifying which parts of the training set would benefit the most, so they can be used as anchor points in the augmentation process. A key assumption in time series forecasting, particularly in few-shot learning scenarios, is that forecasting models tend to overfit certain regions of the training data. Different training samples can have varying impacts on training quality. Intuitively, we aim to generate new data with distributions around the original data points that have higher probabilities of overfitting. To achieve this, we measure the cross-validation errors from a batch of forecasting models to pinpoint the overfit-prone samples.

To construct the forecasting model zoo, we divide the training set into k parts and perform k -fold cross-validation. In this way, we obtain k sets of model parameters for the same network architecture, *e.g.*, *iTransformer* [21], which we denote as \mathcal{M} . For each data point x , we evaluate the prediction errors of the other $k - 1$ models that were not trained on this subset, along with the training error of the model trained on this subset. We then calculate the variance of the MSE across the k models, denoted as $\text{Var}(x; \mathcal{M})$, and sort the “model-zoo variance” of all data points.

The model-zoo variance measures the inconsistency in predictions made by different models trained on slightly different subsets, and can therefore serve as an indicator of the overfit-prone samples. When a model overfits, its predictions on certain data points are highly sensitive to the specific subset it was trained on, leading to a high variability of the performance across the k models. As a result, data points with high model-zoo variance are more likely to be in regions where the models struggle to generalize, making them overfit-prone and thus ideal candidates for data augmentation to improve generalization. In practice, we split the training set into two subsets based on the top and bottom 50% values of the model-zoo variance, and refer to the top 50% subset as the overfit-prone samples.

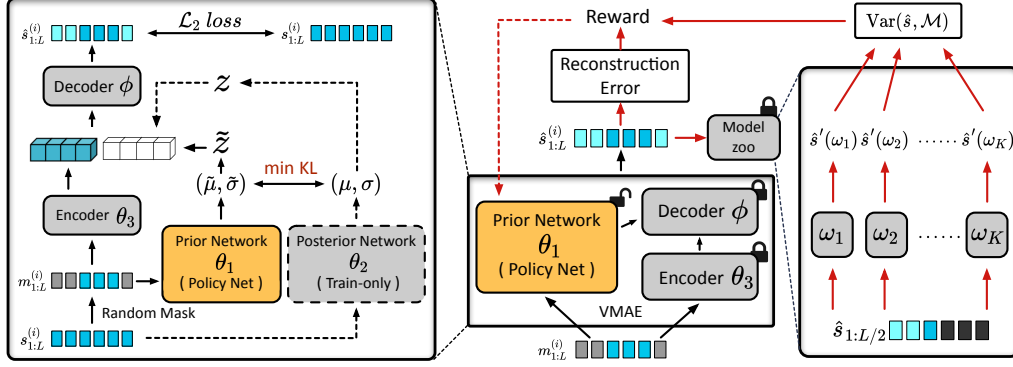


Figure 3: Architecture of ReAugment. **Left:** ReAugment pretrains a VMAE as the augmentation backbone, modeling the original distribution of overfit-prone data. **Right:** An RL framework finetunes the VMAE prior network, using its latent space as the action space, guided by a reward function that promotes diverse sample generation around overfit-prone regions.

3.2 Preliminary Findings on Overfit-Prone Data

To understand the impact of the overfit-prone samples on the training process, we conduct the following experiments. We train forecasting models separately using data from Group A (the subset with the top 50% model-zoo variance) and Group B (the subset with the bottom 50% model-zoo variance). We evaluate the models on the same test set. Given its superior average performance, we select iTransformer as the preferred model for these experiments. The experiments are conducted on classic real-world multivariate benchmarks, including *ETT*, *Weather*, and *Electricity*. The forecasting results are shown in Figure 2, where a lower MAE indicates more accurate predictions. Our experiments demonstrate that the choice of training sets significantly impacts final performance. Predictions trained in Group B consistently outperform those trained in Group A across all benchmarks, with substantial margins. This finding suggests that the overfit-prone samples are more likely to negatively affect the training quality of forecasting models. Since data augmentation is an effective strategy to mitigate overfitting, we propose generating new data around the distributions of the overfit-prone samples, allowing the forecasting model to learn more generalizable patterns from these data points.

4 ReAugment

4.1 Overall Training Pipeline

Based on preliminary findings regarding overfit-prone data, we recognize the importance of identifying such samples and using them as anchor points for data augmentation. This approach can help prevent the model from overfitting to specific patterns. By doing so, our method effectively tackles the challenges of data scarcity, leading to improved generalization performance in few-shot learning scenarios. The training pipeline of our approach consists of three stages:

- Stage A: Train a probabilistic generative model to initialize the neural augmentor using overfit-prone samples. Implemented as a VMAE, the model takes partially masked time series data and corresponding absolute timestamps in the dataset as inputs to reconstruct the complete data.
- Stage B: Finetune the VMAE using an RL algorithm, enabling it to generate augmented data that goes beyond merely replicating the original data distribution.
- Stage C: Train the forecasting model using both the original and the augmented data.

Specifically, we augment the top 50% overfit-prone samples, tripling the size of the original training set. This pipeline ensures that data augmentation targets overfit-prone samples, addressing their weaknesses and improving forecasting model performance in data-scarce scenarios.

4.2 Variational Masked Autoencoder as the RL Actor

By using a probabilistic generative model as the neural augmentor, denoted as $\hat{s}_{1:L}^{(i)} \sim G(s_{1:L}^{(i)}, z^{(i)})$, we can generate an infinite amount of data by learning a transformation function based on the overfit-prone data $s_{1:L}^{(i)}$, where i is the data index and L is the length of the data sequence. The key is to learn an appropriate distribution of the latent variable z , balancing the diversity of the augmented data with

its similarity to the original data. For simplicity, we omit the data index in the following notations. The initial learning step involves optimizing G with a data reconstruction objective, minimizing the divergence between the masked data and the original data distribution.

We design a Variational Masked Autoencoder (VMAE), as illustrated in Figure 3(left), which takes masked time series data $m_{1:L}$ with absolute timestamp $t_{1:L}$ in the whole dataset as input and outputs the complete corresponding data. The entire architecture contains four modules, including (i) the prior network, which learns the prior distribution of z based on the masked data, (ii) the posterior module, which learns the posterior distribution of z based on the original data, (iii) the data encoder, which extracts significant features from $m_{1:L}$ with $t_{1:L}$, (iv) the decoder, which generates data from the encoding features and the latent variables. These modules are parametrized by $\theta_{1:3}$ and ϕ :

$$\begin{aligned} \text{Prior: } \tilde{z} &\sim p(m_{1:L}, t_{1:L}; \theta_1), & \text{Posterior: } z &\sim q(s_{1:L}, t_{1:L}; \theta_2), \\ \text{Encoder: } u &= \text{Enc}(m_{1:L}, t_{1:L}; \theta_3), & \text{Decoder: } \hat{s}_{1:L} &= \text{Dec}(\text{concat}(u, z); \phi). \end{aligned} \quad (1)$$

We draw the latent variables, which control the diversity of the generated data, from parametrized Gaussian distributions. The mean and standard deviation of these distributions are produced by the prior and posterior modules. We minimize the Kullback–Leibler (KL) divergence between the prior and posterior distributions. After this training stage, we replace the posterior z with the prior \tilde{z} as input to the decoder. The overall objective function is

$$\mathcal{L} = \mathbb{E}_{s \sim D_s} \|\hat{s}_{1:L} - s_{1:L}\|_2^2 + \beta \mathcal{D}_{KL}(q(z | s_{1:L}, t_{1:L}) \| p(\tilde{z} | m_{1:L}, t_{1:L})), \quad (2)$$

where D_s is the set of the overfit-prone data obtained by measuring the prediction diversity over the model zoo. In line with previous work, we use the \mathcal{L}_2 loss to measure the reconstruction error. Notably, the posterior module is used exclusively to constrain the prior learner and is not utilized in subsequent training stages.

A key aspect of our method is how we handle the absolute timestamps $t_{1:L}$ during the training and data augmentation phases, respectively. While VMAE is initially trained using the original absolute timestamps from the data, during the data augmentation phase in Stages B&C, we modify these timestamps by sampling them from the test set’s time range, rather than from the training time range. Empirically, this technique allows us to generate augmented samples that are more closely aligned with the distribution of the test set.

In general, the VMAE design can be integrated into any encoder-decoder-based time series forecasting architecture. In this work, we specifically adopt the encoder and decoder (implemented as a linear projector) from iTransformer [21] for feature extraction and decoding.

4.3 Variance-Guided REINFORCE Using Model Zoo Predictions

Motivation: Few-shot time series forecasting is particularly prone to distribution imbalance and shifts, leading to sparse regions that increase overfitting risk. Thus, merely replicating the original data distribution in Stage B is insufficient. To address this, we propose an RL-based framework to expand the distribution around overfit-prone samples, aiming to better cover test patterns and avoid trivial solutions. The augmented data should (i) *increase diversity near overfit-prone regions*, and (ii) *remain close to the original distribution to avoid noise*. Inspired by our findings, we achieve this by augmenting samples that show diverse predictions across the model zoo. The key insight is to effectively use the potentially overfit-prone data to strengthen generalization.

Intuitively, the variance of prediction errors across the model zoo reflects the degree of overfitting at a given data point. The model zoo \mathcal{M} consists of K network instances of the same network architecture with pretrained parameters $\omega_{1:K}$, constructed via K -fold cross-validation. Each data sample is used as test data for one model and as training data for the other $K - 1$ models. We estimate overfitting at each training sequence by computing the variance of prediction errors across the $K - 1$ models that were trained on it. Similarly, for the augmented data $\hat{s}_{1:L}$, we compute the *model-zoo variance* by

$$\begin{aligned} \text{Var}(\hat{s}_{1:L}, \mathcal{M}) &= \frac{1}{K-1} \sum_1^{K-1} (\|\hat{s}_{L/2:L} - \hat{s}'_{L/2:L}(\omega_k)\|_2^2 - \bar{e})^2, \\ \text{s.t. } \bar{e} &= \frac{1}{K-1} \sum_1^{K-1} \|\hat{s}_{L/2:L} - \hat{s}'_{L/2:L}(\omega_k)\|_2^2, \end{aligned} \quad (3)$$

where $\hat{s}'_{L/2:L}(\omega_k)$ represents the prediction result from the k -th forecasting model. However, a practical challenge is that the *model-zoo variance* is **non-differentiable**, preventing direct gradient-based optimization of the augmentor. To address this, we finetune the neural augmentor using the REINFORCE algorithm, treating the latent space from the VMAE prior module as the action space. Specifically, we optimize the prior module as a policy network while keeping other components fixed, aiming to maximize the following reward function:

$$r = \frac{1}{1 + e^{-\eta \cdot f(\hat{s}_{1:L}, \mathcal{M})}}, \quad \text{s.t.} \quad f(\hat{s}_{1:L}, \mathcal{M}) = \frac{\text{Var}(\hat{s}_{1:L}, \mathcal{M})}{\|\hat{s}_{1:L} - s_{1:L}\|_2^2}. \quad (4)$$

Based on this reward function, the policy network (*i.e.*, the prior network in VMAE) is optimized as follows via gradient ascent, where α is the learning rate: $\theta_1 \leftarrow \theta_1 + \alpha \cdot r \cdot \nabla_{\theta_1} \log p(\tilde{z} \mid m_{1:L}, t_{1:L}; \theta_1)$. The reward function encourages augmented samples to exhibit more pronounced predictive variance across the model zoo, while also constraining the differences between the augmented and original data. In the reward function, a scaled-sigmoid function is employed to minimize the likelihood of rewards clustering around 0 or 1 controlled by the hyperparameter η . This approach ensures that, despite potential order-of-magnitude differences in reconstruction error and backtest variance within the model zoo, the reward function can learn effectively from these variations.

5 Experiments

5.1 Experimental Setups

Following previous work [33, 21, 23, 38], we thoroughly evaluate the proposed ReAugment on five publicly available real-world datasets: *ETT* (including 4 subsets), *Traffic*, *Electricity*, *Weather*, and *Exchange*. Please refer to Suppl. B for more details on these datasets. We evaluate ReAugment in two setups: the few-shot setup and the standard setup, which provides full access to the original training set of the above datasets.

- *Few-shot setup*: we simulate scenarios with limited training data to assess the model’s ability to handle data scarcity. We reduce the training set size to either 10% or 20% of the full dataset, depending on the dataset characteristics. The few-shot training data corresponds to the earliest portion of the time series, ensuring a significant distribution shift from the test set. The validation and test sets remain consistent with those used in prior studies.
- *Standard setup*: We follow the configuration from previous work, allowing access to the full training set while keeping the validation and test sets unchanged.

We employ a fixed lookback length of 96 time steps across all datasets and report the multivariate sequence prediction results with prediction lengths of 96 time steps. We provide additional implementation details in Suppl. C, including information on hyperparameters and sensitivity analysis.

Forecasting model backbones. We primarily use iTransformer [21] for the forecasting model, as it has demonstrated strong performance in standard time series forecasting tasks. We also conduct experiments with another Transformer-based method, PatchTST [23], and the linear model DLinear [38]. Unless otherwise specified, we use a model zoo consisting of 4 cross-validation models.

Compared methods. We compare ReAugment with the following augmentation methods:

- *Gaussian augmentation*: Inspired by prior literature [13], we use traditional data augmentation methods that apply simple transformations, such as adding Gaussian noise to the raw data. This approach enhances the diversity of the training data by adjusting the controllable variances and means of the added Gaussian noise.
- *Convolve*: We employ another traditional data augmentation method based on the Convolve function in the *Tsaug* library [31].
- *TimeGAN* [36]: TimeGAN data augmentor combines supervised and adversarial objective optimization. Specifically, through a learned embedding space, the network is guided to adhere to the dynamics of the training data during sampling.
- *ADA* [26]: We employ the Anchor Data Augmentation (ADA) method, which improves the domain-agnostic Mixup techniques. ADA uses multiple replicas of modified samples generated by Anchor Regression to create additional training examples.

Table 1: The impact of ReAugment on different forecasting models in the few-shot setup. The augmentor is trained with three different random seeds. We report the average results of each model across different augmented datasets and include the standard deviation results in Suppl. D.

Training Data	iTransformer		PatchTST		DLinear		Average	
	MAE	MSE	MAE	MSE	MAE	MSE	MAE	MSE
ETTh1 (Raw)	0.434	0.411	0.458	0.446	0.435	0.408	0.442	0.422
+ ReAugment	0.422	0.403	0.440	0.429	0.422	0.388	0.428	0.407
Promotion	2.76%	1.95%	3.93%	3.81%	2.99%	4.90%	3.23%	3.55%
ETTh2 (Raw)	0.362	0.320	0.367	0.321	0.402	0.356	0.377	0.332
+ ReAugment	0.339	0.302	0.349	0.306	0.369	0.334	0.352	0.310
Promotion	6.35%	5.63%	4.90%	4.67%	8.21%	6.18%	6.49%	5.49%
ETTm1 (Raw)	0.440	0.470	0.428	0.457	0.442	0.471	0.437	0.466
+ ReAugment	0.410	0.436	0.403	0.433	0.431	0.462	0.415	0.444
Promotion	6.82%	7.23%	5.84%	5.25%	2.49%	1.91%	5.05%	4.80%
ETTm2 (Raw)	0.282	0.204	0.276	0.199	0.303	0.219	0.287	0.207
+ ReAugment	0.275	0.196	0.268	0.193	0.297	0.216	0.280	0.202
Promotion	2.48%	3.92%	2.90%	3.02%	1.98%	1.37%	2.45%	2.77%
Weather (Raw)	0.231	0.187	0.232	0.189	0.277	0.212	0.247	0.196
+ ReAugment	0.229	0.185	0.227	0.186	0.276	0.212	0.244	0.194
Promotion	0.87%	1.07%	2.16%	1.59%	0.36%	0.00%	1.13%	0.89%
Electricity (Raw)	0.258	0.168	0.295	0.200	0.307	0.215	0.287	0.194
+ ReAugment	0.254	0.165	0.275	0.187	0.305	0.216	0.278	0.189
Promotion	1.55%	1.79%	6.78%	6.50%	0.65%	-0.47%	2.99%	2.61%
Traffic (Raw)	0.318	0.466	0.327	0.541	0.452	0.724	0.366	0.578
+ ReAugment	0.293	0.429	0.314	0.521	0.406	0.663	0.338	0.538
Promotion	7.86%	7.94%	3.98%	3.70%	10.18%	8.43%	7.34%	6.69%
Exchange (Raw)	0.228	0.103	0.226	0.103	0.226	0.104	0.227	0.103
+ ReAugment	0.224	0.097	0.223	0.098	0.224	0.099	0.224	0.098
Promotion	1.75%	5.83%	1.33%	4.85%	0.88%	4.81%	1.32%	5.16%

Table 2: The few-shot forecasting performance using different data augmentation methods. We use iTransformer as the forecasting model and employ the same random seeds for training. For ReAugment, which leverages a stochastic data augmentor, we train the model three times with different augmentation sets and report the mean and standard deviation of the results.

Dataset	Original		Gaussian		Convolve		TimeGAN		ADA		ReAugment	
	MAE	MSE	MAE	MSE	MAE	MSE	MAE	MSE	MAE	MSE	MAE	MSE
ETTh1	0.434	0.411	0.437	0.416	0.441	0.417	0.444	0.419	0.435	0.413	0.422 ± 0.01	0.403 ± 0.01
ETTh2	0.362	0.320	0.365	0.321	0.364	0.323	0.366	0.327	0.368	0.331	0.339 ± 0.01	0.302 ± 0.01
ETTm1	0.440	0.470	0.438	0.469	0.426	0.479	0.430	0.483	0.429	0.484	0.410 ± 0.01	0.436 ± 0.01
ETTm2	0.282	0.204	0.283	0.204	0.286	0.207	0.285	0.206	0.284	0.207	0.275 ± 0.02	0.196 ± 0.01
Weather	0.231	0.187	0.240	0.196	0.253	0.204	0.239	0.191	0.246	0.198	0.229 ± 0.00	0.185 ± 0.00
Electricity	0.258	0.168	0.263	0.170	0.262	0.170	0.267	0.177	0.265	0.171	0.254 ± 0.01	0.165 ± 0.01
Traffic	0.318	0.466	0.319	0.467	0.320	0.463	0.315	0.449	0.318	0.456	0.293 ± 0.01	0.429 ± 0.01
Exchange	0.228	0.103	0.229	0.104	0.226	0.099	0.226	0.100	0.235	0.116	0.224 ± 0.00	0.097 ± 0.00

5.2 Results of Few-Shot Time Series Forecasting

Under the few-shot setup, we evaluate the effectiveness of ReAugment on various forecasting models, including iTransformer [21], PatchTST [23], and DLinear [38]. As shown in Table 1, our method consistently improves prediction accuracy across various public datasets when applied to different forecasting models, demonstrating its adaptability and effectiveness in automated data augmentation. Moreover, the proposed reward formulation in the REINFORCE stage further enhances performance, showing robustness across model zoo configurations. Therefore, ReAugment serves not just as a fixed augmentation scheme, but as a flexible design paradigm adaptable to different tasks and objectives. Table 2 compares the performance of various augmentation methods, all using iTransformer as the forecasting model and tripling the size of the original training set.

Table 3: The performance of ReAugment under standard setup with full training set. Like previous experiments, we use iTransformer as the forecasting model and employ the same random seeds.

Dataset	Original		Guassian		Convolve		TimeGAN		ADA		ReAugment	
	MAE	MSE	MAE	MSE	MAE	MSE	MAE	MSE	MAE	MSE	MAE	MSE
ETTh1	0.405	0.387	0.407	0.392	0.416	0.399	0.409	0.390	0.407	0.391	0.396 ± 0.01	0.381 ± 0.01
ETTh2	0.350	0.301	0.352	0.307	0.356	0.303	0.348	0.299	0.347	0.297	0.346 ± 0.01	0.294 ± 0.01
ETTm1	0.377	0.341	0.374	0.340	0.387	0.352	0.392	0.357	0.372	0.336	0.364 ± 0.01	0.328 ± 0.01
ETTm2	0.272	0.186	0.272	0.187	0.275	0.188	0.279	0.190	0.273	0.188	0.263 ± 0.01	0.179 ± 0.00
Weather	0.219	0.178	0.227	0.187	0.265	0.210	0.219	0.177	0.222	0.180	0.206 ± 0.00	0.170 ± 0.00
Electricity	0.239	0.148	0.243	0.150	0.264	0.170	0.276	0.183	0.241	0.149	0.236 ± 0.01	0.147 ± 0.01
Traffic	0.269	0.392	0.269	0.394	0.283	0.407	0.296	0.412	0.268	0.391	0.264 ± 0.01	0.388 ± 0.01
Exchange	0.206	0.086	0.208	0.087	0.210	0.087	0.210	0.087	0.209	0.087	0.204 ± 0.00	0.085 ± 0.00

Table 4: \mathcal{F}_{MAE} and \mathcal{F}_{MSE} results. These metrics assess the relative improvements in performance achieved by data augmentation in the few-shot setup, compared to using the full training set.

Dataset	Gaussian		Convolve		TimeGAN		ADA		ReAugment	
	\mathcal{F}_{MAE}	\mathcal{F}_{MSE}	\mathcal{F}_{MAE}	\mathcal{F}_{MSE}	\mathcal{F}_{MAE}	\mathcal{F}_{MSE}	\mathcal{F}_{MAE}	\mathcal{F}_{MSE}	\mathcal{F}_{MAE}	\mathcal{F}_{MSE}
ETTh1	-10.3%	-20.8%	-24.1%	-25%	-34.5%	-33.3%	-3.4%	-8.3%	41.4%	33.3%
ETTh2	-25%	-5.3%	-16.7%	-15.8%	-33.3%	-36.8%	-50.0%	-57.9%	191.7%	94.7%
ETTm1	3.2%	0.8%	22.2%	-7.0%	15.9%	-10.1%	17.5%	-10.8%	47.6%	26.4%
ETTm2	-10.0%	0.0%	-40.0%	-16.7%	-30.0%	-11.1%	-20.0%	-16.7%	70.0%	44.4%
Weather	-75.0%	-100.0%	-183.3%	-188.9%	-66.7%	-44.4%	-125%	-122.2%	16.7%	22.2%
Elec.	-26.3%	-10.0%	-21.1%	-10.0%	-47.4%	-45.0%	-36.8%	-15.0%	21.1%	15.0%
Traffic	-2.0%	-1.4%	-4.1%	4.1%	6.1%	23.0%	0.0%	13.5%	51.5%	50.0%
Exc.	-4.5%	-5.9%	9.1%	23.5%	9.1%	17.6%	-31.8%	-76.5%	18.2%	35.3%

5.3 Results with Full Access to Training Set

ReAugment can also be applied to standard time series forecasting scenarios, where we have full access to the entire training sets. As shown in Table 3, ReAugment delivers significant performance improvements across multiple datasets in the standard setup, highlighting its strong generalizability beyond the few-shot learning context. Other experimental details, such as the lookback and prediction lengths, are consistent with those in the few-shot setup.

5.4 Model Analyses

A new evaluation metric for augmentation. Evaluating the improved forecasting accuracy achieved through data augmentation provides a direct measure of our method’s effectiveness. However, it does not account for the fact that the impact of data scarcity can vary significantly across different datasets. We propose a new metric that calculates the ratio of the performance promotion achieved through data augmentation in the few-shot setup, compared to the improvement obtained using the full training set. For example, when using MSE, it can be formulated as $\mathcal{F}_{MSE} = \frac{1 - \text{MSE}_{\text{augment}} / \text{MSE}_{\text{few-shot}}}{1 - \text{MSE}_{\text{standard}} / \text{MSE}_{\text{few-shot}}}$. This metric considers the nature of the dataset and provides a more comprehensive evaluation of the value of augmentation. As shown in Table 4, a larger value indicates a greater performance improvement due to data augmentation.

Ablation study on REINFORCE. The proposed RL framework enables our model to optimize the distribution of the latent variable z based on the backtest results across the model zoo, thereby generating augmented data that balances data diversity and similarity to the original data. However, without RL finetuning, the original VMAE model can also be used as an independent data augmentor. Accordingly, we train the iTransformer model using augmented data by the VMAE model pretrained in Stage A. As shown in Table 5, the use of RL consistently improves the prediction results in most cases, highlighting the significance of RL finetuning for improving the quality of the augmented data.

Shall we augment all training samples? Inspired by preliminary findings, we augment the top 50% overfit-prone samples. What would be the impact of augmenting more or fewer samples? To investigate this, we compare augmenting different proportions of overfit-prone samples with augmenting the entire few-shot dataset. For consistency, the total amount of augmented data was kept three times the size of the original training set and applied to the iTransformer model. As shown

Table 5: Ablation studies on the impact of the REINFORCE algorithm under the few-shot forecasting setup. For both models without or with RL, we use augmented data, three times the amount of the original data, to train the forecasting iTransformer.

RL	ETTh1		ETTh2		ETTm1		ETTm2		Weather		Electricity		Traffic	
	MAE	MSE	MAE	MSE	MAE	MSE	MAE	MSE	MAE	MSE	MAE	MSE	MAE	MSE
×	0.424	0.404	0.341	0.304	0.416	0.441	0.276	0.196	0.230	0.186	0.255	0.166	0.292	0.430
✓	0.422	0.403	0.339	0.302	0.410	0.436	0.275	0.196	0.229	0.185	0.254	0.165	0.293	0.429

Table 6: An analysis of the overfit-prone samples used as augmentation anchor points in ReAugment. Overfit-prone samples refer to training data with the highest variance in prediction errors across the forecasting model zoo. We compare the performance of different iTransformer models trained with subsets that retain different ratios of these overfit-prone samples. For all comparison models, we generate augmented data three times the size of the entire few-shot training set.

Augmented Data	ETTh1		ETTh2		ETTm1		ETTm2		Weather	
	MAE	MSE	MAE	MSE	MAE	MSE	MAE	MSE	MAE	MSE
10% Top-Variance Data	0.431	0.409	0.341	0.305	0.422	0.445	0.277	0.199	0.229	0.185
30% Top-Variance Data	0.426	0.408	0.339	0.303	0.415	0.441	0.265	0.184	0.228	0.183
50% Top-Variance Data	0.422	0.403	0.339	0.302	0.410	0.436	0.275	0.196	0.229	0.185
70% Top-Variance Data	0.424	0.405	0.345	0.307	0.421	0.446	0.274	0.193	0.230	0.186
All Training Data	0.436	0.412	0.351	0.311	0.433	0.460	0.283	0.203	0.233	0.188

in Table 6, directly augmenting the entire few-shot dataset was less effective than data-dependent augmentation, which aligns with our preliminary findings. Furthermore, augmenting different percentages of high-variance samples resulted in varying degrees of improvement, demonstrating that our data augmentation model can adaptively enhance overfit-prone samples, leading to better performance of the forecasting model.

Computational costs. Table 7 reports the training time for VMAE, REINFORCE, and the forecasting model in the few-shot setting. The added time from Stages A and B is acceptable given the performance gains and remains shorter than training the forecasting models. All experiments are conducted on an NVIDIA RTX 3090 GPU.

Hyperparameters. In Suppl. C, we conduct sensitivity analyses on the size of the model zoo (K) and the mask rate of VMAE, and present details of other hyperparameters in our model.

Table 7: Computational cost for each training stage. The total training time required for dataset augmentation, including Stage A and Stage B, is notably shorter than the time needed for training the forecasting models, indicating our method’s reasonable efficiency.

Dataset	Stage A: VMAE	Stage B: REINFORCE	Stage C: Forecasting	
			iTransformer	PatchTST
ETTh1	1min	2min	2min	5min
Elec.	24min	31min	1h 33min	2h 24min
Traffic	1h 22min	1h 53min	4h 27min	6h 50min

6 Conclusions and Limitations

In this paper, we proposed ReAugment, a novel data augmentation method driven by reinforcement learning. Key technical contributions include: (i) Identifying overfit-prone data samples that could significantly benefit from augmentation by assessing their prediction diversity across a forecasting model zoo; (ii) Training a variational generative model within an RL framework to transform these overfit-prone samples into new data points, guided by a reward function derived from the performance of the model zoo, thereby enhancing both the quality and diversity of the augmented data. ReAugment significantly boosts forecasting performance while maintaining minimal computational overhead by leveraging a learnable policy to transform the overfit-prone samples.

One unresolved issue in this study is the reliance on multiple pretrained models. The proposed method introduces additional computational overhead due to the need for training VMAE, applying

the REINFORCE algorithm, and performing backtesting across the model zoo. We provide a detailed comparison of the computational costs for each training stage in the experimental section.

References

- [1] Bian, Y., Ju, X., Li, J., Xu, Z., Cheng, D., and Xu, Q. Multi-patch prediction: Adapting llms for time series representation learning. In *ICML*, 2024.
- [2] Cao, D., Jia, F., Arik, S. O., Pfister, T., Zheng, Y., Ye, W., and Liu, Y. Tempo: Prompt-based generative pre-trained transformer for time series forecasting. In *ICLR*, 2024.
- [3] Cao, P., Li, X., Mao, K., Lu, F., Ning, G., Fang, L., and Pan, Q. A novel data augmentation method to enhance deep neural networks for detection of atrial fibrillation. *Biomedical Signal Processing and Control*, 56:101675, 2020.
- [4] Che, Z., Purushotham, S., Cho, K., Sontag, D., and Liu, Y. Recurrent neural networks for multivariate time series with missing values. *Scientific Reports*, 8(1):6085, 2018.
- [5] Cheung, T.-H. and Yeung, D.-Y. Modals: Modality-agnostic automated data augmentation in the latent space. In *ICLR*, 2020.
- [6] Cui, X., Goel, V., and Kingsbury, B. Data augmentation for deep neural network acoustic modeling. *IEEE/ACM Transactions on Audio, Speech, and Language Processing*, 23(9):1469–1477, 2015.
- [7] Das, A., Kong, W., Sen, R., and Zhou, Y. A decoder-only foundation model for time-series forecasting. In *ICML*, 2024.
- [8] Demirel, B. U. and Holz, C. Finding order in chaos: A novel data augmentation method for time series in contrastive learning. In *NeurIPS*, volume 36, 2024.
- [9] Dooley, S., Khurana, G. S., Mohapatra, C., Naidu, S. V., and White, C. Forecastpfn: Synthetically-trained zero-shot forecasting. In *NeurIPS*, 2023.
- [10] Ekambaram, V., Jati, A., Dayama, P., Mukherjee, S., Nguyen, N. H., Gifford, W. M., Reddy, C., and Kalagnanam, J. Tiny time mixers (ttms): Fast pre-trained models for enhanced zero/few-shot forecasting of multivariate time series. In *NeurIPS*, 2024.
- [11] Flores, A., Tito-Chura, H., and Apaza-Alanoca, H. Data augmentation for short-term time series prediction with deep learning. In *Intelligent Computing: Proceedings of the 2021 Computing Conference*, pp. 492–506, 2021.
- [12] Huang, H., Chen, M., and Qiao, X. Generative learning for financial time series with irregular and scale-invariant patterns. In *ICLR*, 2023.
- [13] Iglesias, G., Talavera, E., González-Prieto, Á., Mozo, A., and Gómez-Canaval, S. Data augmentation techniques in time series domain: a survey and taxonomy. *Neural Computing and Applications*, 35(14): 10123–10145, 2023.
- [14] Jiang, X., Missel, R., Li, Z., and Wang, L. Sequential latent variable models for few-shot high-dimensional time-series forecasting. In *The Eleventh International Conference on Learning Representations*, 2023.
- [15] Jin, M., Wang, S., Ma, L., Chu, Z., Zhang, J. Y., Shi, X., Chen, P.-Y., Liang, Y., Li, Y.-F., Pan, S., et al. Time-llm: Time series forecasting by reprogramming large language models. In *ICLR*, 2024.
- [16] Li, L., Yan, J., Wang, H., and Jin, Y. Anomaly detection of time series with smoothness-inducing sequential variational auto-encoder. *IEEE Transactions on Neural Networks and Learning Systems*, 32(3):1177–1191, 2020.
- [17] Li, S., Jin, X., Xuan, Y., Zhou, X., Chen, W., Wang, Y.-X., and Yan, X. Enhancing the locality and breaking the memory bottleneck of transformer on time series forecasting. In *NeurIPS*, volume 32, 2019.
- [18] Liao, S., Ni, H., Szpruch, L., Wiese, M., Sabate-Vidales, M., and Xiao, B. Conditional sig-wasserstein gans for time series generation. *arXiv preprint arXiv:2006.05421*, 2020.
- [19] Liu, H., Zhao, Z., Wang, J., Kamarthi, H., and Prakash, B. A. Lstprompt: Large language models as zero-shot time series forecasters by long-short-term prompting. In *ACL finding*, 2024.

- [20] Liu, S., Yu, H., Liao, C., Li, J., Lin, W., Liu, A. X., and Dustdar, S. Pyraformer: Low-complexity pyramidal attention for long-range time series modeling and forecasting. In *ICLR*, 2021.
- [21] Liu, Y., Hu, T., Zhang, H., Wu, H., Wang, S., Ma, L., and Long, M. itransformer: Inverted transformers are effective for time series forecasting. In *ICLR*, 2024.
- [22] Liu, Y., Zhang, H., Li, C., Huang, X., Wang, J., and Long, M. Timer: Generative pre-trained transformers are large time series models. In *ICML*, 2024.
- [23] Nie, Y., Nguyen, N. H., Sinthong, P., and Kalagnanam, J. A time series is worth 64 words: Long-term forecasting with transformers. In *ICLR*, 2023.
- [24] Pan, Z., Jiang, Y., Garg, S., Schneider, A., Nevmyvaka, Y., and Song, D. s^2ip -llm: Semantic space informed prompt learning with llm for time series forecasting. In *ICML*, 2024.
- [25] Sagheer, A. and Kotb, M. Time series forecasting of petroleum production using deep lstm recurrent networks. *Neurocomputing*, 323:203–213, 2019.
- [26] Schneider, N., Goshtasbpour, S., and Perez-Cruz, F. Anchor data augmentation. In *NeurIPS*, volume 36, 2024.
- [27] Sohn, K., Lee, H., and Yan, X. Learning structured output representation using deep conditional generative models. In *NeurIPS*, volume 28, 2015.
- [28] Torres, J. F., Hadjout, D., Sebaa, A., Martínez-Álvarez, F., and Troncoso, A. Deep learning for time series forecasting: a survey. *Big Data*, 9(1):3–21, 2021.
- [29] Wang, H., Peng, J., Huang, F., Wang, J., Chen, J., and Xiao, Y. Micn: Multi-scale local and global context modeling for long-term series forecasting. In *ICLR*, 2022.
- [30] Wen, Q., Sun, L., Yang, F., Song, X., Gao, J., Wang, X., and Xu, H. Time series data augmentation for deep learning: A survey. In *IJCAI*, 2021.
- [31] Wen, T. and Keyes, R. Time series anomaly detection using convolutional neural networks and transfer learning. *arXiv preprint arXiv:1905.13628*, 2019.
- [32] Williams, R. J. Simple statistical gradient-following algorithms for connectionist reinforcement learning. *Machine Learning*, 8:229–256, 1992.
- [33] Wu, H., Xu, J., Wang, J., and Long, M. Autoformer: Decomposition transformers with auto-correlation for long-term series forecasting. In *NeurIPS*, volume 34, pp. 22419–22430, 2021.
- [34] Xu, J., Li, K., and Li, D. An automated few-shot learning for time-series forecasting in smart grid under data scarcity. *IEEE Transactions on Artificial Intelligence*, 5(6):2482–2492, 2024.
- [35] Yi, K., Zhang, Q., Fan, W., Wang, S., Wang, P., He, H., An, N., Lian, D., Cao, L., and Niu, Z. Frequency-domain mlps are more effective learners in time series forecasting. In *NeurIPS*, volume 36, 2024.
- [36] Yoon, J., Jarrett, D., and Van der Schaar, M. Time-series generative adversarial networks. In *NeurIPS*, volume 32, 2019.
- [37] Yuan, Y., Shao, C., Ding, J., Jin, D., and Li, Y. Spatio-temporal few-shot learning via diffusive neural network generation. In *ICLR*, 2024.
- [38] Zeng, A., Chen, M., Zhang, L., and Xu, Q. Are transformers effective for time series forecasting? In *AAAI*, volume 37, pp. 11121–11128, 2023.
- [39] Zhang, Y. and Yan, J. Crossformer: Transformer utilizing cross-dimension dependency for multivariate time series forecasting. In *ICLR*, 2022.
- [40] Zhou, H., Zhang, S., Peng, J., Zhang, S., Li, J., Xiong, H., and Zhang, W. Informer: Beyond efficient transformer for long sequence time-series forecasting. In *AAAI*, volume 35, pp. 11106–11115, 2021.
- [41] Zhou, T., Ma, Z., Wen, Q., Wang, X., Sun, L., and Jin, R. Fedformer: Frequency enhanced decomposed transformer for long-term series forecasting. In *ICML*, pp. 27268–27286, 2022.

Supplementary Material

A Overall Training Pipeline

We present the overall training pipeline in Algorithm 1.

Algorithm 1 Overall training pipeline

- 1: **Given:** Time series samples from training set $s_{1:L}^{(i)}$
 - 2: **Key problem:** Which samples should be augmented and how to augment them?
 - 3: // Stage A: Train the VMAE supervised by original data
 - 4: VMAE can be parameterized as $\theta_1, \theta_2, \theta_3, \phi$, all parameters are optimized during the training phase.
 - 5: // Stage B: Data filtering by model zoo variance
 - 6: Pretrain a model zoo and assess on the training set.
 - 7: The top 50% samples with large variance on the model zoo are found from the training set and formulated as $s_{1:L}$.
 - 8: // REINFORCE with model zoo
 - 9: Fixed parameters θ_2, θ_3, ϕ .
 - 10: **while** not converged **do**
 - 11: Sample batch of time series samples and mask randomly, formulated as $m_{1:L}$.
 - 12: Input masked data $m_{1:L}$ to pretrained VMAE, calculate the reward r by the output of VMAE and pretrained model zoo.
 - 13: Update the policy net parameters:
$$\theta_1 \leftarrow \theta_1 + \alpha \cdot r \cdot \nabla_{\theta_1} \log E_{\theta_1}(\tilde{\mathbf{z}} \mid m_{1:L}, t)$$
 - 14: **end while**
 - 15: Stage C: Train the forecasting model
 - 16: Generate augmented data by ReAugment
 - 17: Further train the forecasting model (*e.g.*, iTransformer) using augmented data
-

B Dataset Details

Here is a detailed description of the five experiment datasets:

1. ETT consists of two hourly-level datasets (ETT_h) and two 15-minute-level datasets (ETT_m). Each of them contains 7 factors of electricity transformers, including load and oil temperature from July 2016 to July 2018.
2. Traffic is a collection of road occupancy rates measured by 862 sensors on San Francisco Bay area freeways from January 2015 to December 2016.
3. ECL collects hourly electricity consumption of 321 clients from 2012 to 2014.
4. The Weather dataset includes 21 meteorological indicators, such as air temperature and humidity, recorded 10 minutes from the weather station of the Max Planck Biogeochemistry Institute in 2020.
5. The Exchange dataset records the daily exchange rates of 8 different countries ranging from 1990 to 2016.

For the standard setup, we follow the data processing method of iTransformer, dividing the dataset into training, validation, and test sets, with this partitioning aligned in chronological order.

In addition, to simulate a scenario with limited training data, we propose the few-shot setup. Specifically, we reduce the training set size to either 10% or 20% of the full dataset, while keeping the validation and test sets the same as in the standard setup. Notably, the training data used consists of the most distant portion of the time series relative to the test set, to simulate a more challenging time series forecasting task. In Table 8, we provide the number of variables (*i.e.*, the feature dimension at a single time point) in each dataset, the total number of time points, and the number of time points within each set of the train-validation-test partitions for both standard and few-shot setup.

Table 8: **Details of the datasets.** *Features* denotes the number of data variables in each dataset. *Time points* refers to the total number of time points in the dataset. *Partition* indicates the number of time points allocated to each subset in the (train, validation, test) splits.

	ETTh1 / ETTh2	ETTm1 / ETTm2	Traffic
Features	7	7	862
Time points (Standard)	14307	57507	17451
Time points (Few-shot)	8443	28793	8756
Partition (Standard)	(8545, 2881, 2881)	(34465, 11521, 11521)	(12185, 1757, 3509)
Partition (Few-shot)	(2681, 2881, 2881)	(5751, 11521, 11521)	(3490, 1757, 3509)
	Electricity	Weather	Exchange
Features	321	21	8
Time points (Standard)	26211	52603	7207
Time points (Few-shot)	13136	21071	3528
Partition (Standard)	(18317, 2633, 5261)	(36792, 5271, 10540)	(5120, 665, 1422)
Partition (Few-shot)	(5242, 2633, 5261)	(5260, 5271, 10540)	(1441, 665, 1422)

C Sensitivity Analysis

C.1 Size of Model Zoo K

In the main text, we use $K = 4$. As shown in Table 9, we provide an analysis of the impact of varying K values under the few-shot learning setup. Experiments show that using too few models affects the variance estimation, while using too many models in a few-shot setting leads to insufficient training data for each model, preventing further improvement in the final results. We observe that the model’s performance remains stable when $K \geq 4$.

Table 9: **Performance comparison across different values of K on multiple datasets.**

Dataset	K=3		K=4		K=6		K=8	
	MAE	MSE	MAE	MSE	MAE	MSE	MAE	MSE
ETTh1	0.433	0.412	0.422	0.403	0.424	0.404	0.423	0.403
ETTh2	0.343	0.308	0.339	0.302	0.337	0.301	0.337	0.301
ETTm1	0.429	0.453	0.410	0.436	0.413	0.437	0.411	0.436
ETTm2	0.277	0.198	0.275	0.196	0.274	0.195	0.274	0.194
Weather	0.231	0.186	0.229	0.185	0.229	0.185	0.229	0.186
Electricity	0.256	0.168	0.254	0.165	0.255	0.166	0.254	0.164
Traffic	0.295	0.436	0.293	0.429	0.292	0.427	0.291	0.426
Exchange	0.225	0.100	0.224	0.097	0.224	0.098	0.224	0.097

C.2 Mask Rate of VMAE

The final model uses a mask rate of 0.3, which is kept for all experiments in the main text. As shown in Table 10, we analyze this hyperparameter in a few-shot learning setup.

Table 10: **Performance under different mask rates across datasets.**

Mask rate	0.1		0.3		0.5		0.7	
	MAE	MSE	MAE	MSE	MAE	MSE	MAE	MSE
ETTh1	0.428	0.409	0.422	0.403	0.425	0.406	0.435	0.413
ETTh2	0.353	0.314	0.339	0.302	0.340	0.303	0.342	0.305
ETTm1	0.423	0.448	0.410	0.436	0.408	0.435	0.412	0.439
ETTm2	0.277	0.200	0.275	0.196	0.275	0.195	0.276	0.198
Weather	0.229	0.186	0.229	0.185	0.229	0.185	0.228	0.184

C.3 Additional Hyperparameters

In Table 11, we provide the hyperparameter details of VMAE and REINFORCE. For the encoder and decoder, we adopt the identical hyperparameters as those employed in iTransformer.

Table 11: **Hyperparameters of ReAugment.**

Notation	Hyperparameter	Description
α	0.001	Learning rate of REINFORCE
β	0.1	Weight of KL-divergence in the VMAE loss function
L	96	Time series periods length
η	0.01	Parameters of scaled sigmoid
N	32	Batch size for VMAE training

Table 12: **Impact of ReAugment on different forecasting models in the few-shot learning setup.**

For the raw data baseline, no standard deviation is reported since the forecasting model is trained with a fixed random seed. In contrast, we report both the mean and standard deviation for ReAugment.

Training Data	iTransformer		PatchTST		DLinear	
	MAE	MSE	MAE	MSE	MAE	MSE
ETTh1 (Raw)	0.434	0.411	0.458	0.446	0.435	0.408
+ ReAugment	0.422±0.01	0.403±0.01	0.440±0.02	0.429±0.02	0.422±0.02	0.388±0.01
ETTh2 (Raw)	0.362	0.320	0.367	0.321	0.402	0.356
+ ReAugment	0.339±0.01	0.302±0.01	0.349±0.01	0.306±0.01	0.369±0.01	0.334±0.01
ETTm1 (Raw)	0.440	0.470	0.428	0.457	0.442	0.471
+ ReAugment	0.410±0.01	0.436±0.01	0.403±0.02	0.433±0.02	0.431±0.01	0.462±0.02
ETTm2 (Raw)	0.282	0.204	0.276	0.199	0.303	0.219
+ ReAugment	0.275±0.02	0.196±0.01	0.268±0.01	0.193±0.01	0.297±0.00	0.216±0.00
Weather (Raw)	0.231	0.187	0.232	0.189	0.277	0.212
+ ReAugment	0.229±0.00	0.185±0.00	0.227±0.00	0.186±0.00	0.276±0.01	0.212±0.00
Electricity (Raw)	0.258	0.168	0.295	0.200	0.307	0.215
+ ReAugment	0.254±0.01	0.165±0.01	0.275±0.01	0.187±0.01	0.305±0.01	0.216±0.01
Traffic (Raw)	0.318	0.466	0.327	0.541	0.452	0.724
+ ReAugment	0.293±0.01	0.429±0.01	0.314±0.02	0.521±0.02	0.406±0.01	0.663±0.02
Exchange (Raw)	0.228	0.103	0.226	0.103	0.226	0.104
+ ReAugment	0.224±0.00	0.097±0.00	0.223±0.00	0.098±0.00	0.224±0.00	0.099±0.00

D Full Results with Multiple Training Seeds

In the main text, for all stochastic data augmentation methods, we conducted experiments using three different random seeds and reported the mean performance. It is worth noting that in all experiments, the source of randomness stems solely from the data augmentation methods, rather than the forecasting models. Accordingly, for stochastic augmentation methods, we applied different random seeds during the augmentation process, while keeping the random seed fixed for the training of the forecasting models. Here, we provide the complete results, including both the mean and standard deviation, for the following experiments:

- The impact of ReAugment on different forecasting models under few-shot learning in Table 12;
- The few-shot forecasting performance using different data augmentation methods in Table 13;
- The performance of ReAugment under the standard setup with the full training set in Table 14.

Table 13: **Few-shot forecasting results using various augmentation methods.** We use iTransformer as the forecasting model and report the mean and standard deviation across three random seeds.

Dataset	Original		Gaussian		Convolve	
	MAE	MSE	MAE	MSE	MAE	MSE
ETTh1	0.434	0.411	0.437±0.02	0.416±0.02	0.441±0.03	0.417±0.02
ETTh2	0.362	0.320	0.365±0.01	0.321±0.01	0.364±0.01	0.323±0.01
ETTh1	0.440	0.470	0.438±0.03	0.469±0.02	0.426±0.02	0.479±0.03
ETTh2	0.282	0.204	0.283±0.01	0.204±0.01	0.286±0.01	0.207±0.01
Weather	0.231	0.187	0.240±0.01	0.196±0.00	0.253±0.01	0.204±0.01
Electricity	0.258	0.168	0.263±0.01	0.170±0.01	0.262±0.01	0.170±0.01
Traffic	0.318	0.466	0.319±0.01	0.467±0.02	0.320±0.01	0.463±0.01
Exchange	0.228	0.103	0.229±0.00	0.104±0.00	0.226±0.01	0.099±0.00
Dataset	TimeGAN		ADA		ReAugment	
ETTh1	0.444±0.02	0.419±0.01	0.435±0.01	0.413±0.01	0.422±0.01	0.403±0.01
ETTh2	0.366±0.01	0.327±0.01	0.368±0.00	0.331±0.00	0.339±0.01	0.302±0.01
ETTh1	0.430±0.03	0.483±0.03	0.429±0.01	0.484±0.01	0.410±0.01	0.436±0.01
ETTh2	0.285±0.02	0.206±0.01	0.284±0.01	0.207±0.01	0.275±0.02	0.196±0.01
Weather	0.239±0.01	0.191±0.01	0.246±0.00	0.198±0.00	0.229±0.00	0.185±0.00
Electricity	0.267±0.01	0.177±0.01	0.265±0.01	0.171±0.00	0.254±0.01	0.165±0.01
Traffic	0.315±0.02	0.449±0.03	0.318±0.01	0.456±0.01	0.293±0.01	0.429±0.01
Exchange	0.226±0.01	0.100±0.01	0.235±0.00	0.116±0.00	0.224±0.00	0.097±0.00

Table 14: **Comparison under standard setup with full training set.** We use iTransformer as the forecasting model and report the mean and standard deviation across three random seeds.

Dataset	Original		Gaussian		Convolve	
	MAE	MSE	MAE	MSE	MAE	MSE
ETTh1	0.405	0.387	0.407±0.02	0.392±0.01	0.416±0.03	0.399±0.02
ETTh2	0.350	0.301	0.352±0.01	0.307±0.01	0.356±0.01	0.303±0.01
ETTh1	0.377	0.341	0.374±0.02	0.340±0.02	0.387±0.02	0.352±0.02
ETTh2	0.272	0.186	0.272±0.01	0.187±0.00	0.275±0.01	0.188±0.01
Weather	0.219	0.178	0.227±0.01	0.187±0.01	0.265±0.01	0.210±0.01
Electricity	0.239	0.148	0.243±0.01	0.150±0.00	0.264±0.01	0.170±0.01
Traffic	0.269	0.392	0.269±0.01	0.394±0.02	0.283±0.02	0.407±0.02
Exchange	0.206	0.086	0.208±0.00	0.087±0.00	0.210±0.01	0.087±0.00
Dataset	TimeGAN		ADA		ReAugment	
ETTh1	0.409±0.02	0.390±0.02	0.407±0.01	0.391±0.01	0.396±0.01	0.381±0.01
ETTh2	0.348±0.01	0.299±0.01	0.347±0.00	0.297±0.00	0.346±0.01	0.294±0.01
ETTh1	0.392±0.02	0.357±0.03	0.372±0.01	0.336±0.02	0.364±0.01	0.328±0.01
ETTh2	0.279±0.01	0.190±0.01	0.273±0.00	0.188±0.00	0.263±0.01	0.179±0.00
Weather	0.219±0.01	0.177±0.01	0.222±0.00	0.180±0.00	0.206±0.00	0.170±0.00
Electricity	0.276±0.02	0.183±0.01	0.241±0.01	0.149±0.01	0.236±0.01	0.147±0.01
Traffic	0.296±0.02	0.412±0.03	0.268±0.02	0.391±0.02	0.264±0.01	0.388±0.01
Exchange	0.210±0.01	0.087±0.00	0.209±0.00	0.087±0.00	0.204±0.00	0.085±0.00